The Janelia Atalanta plasmids provide a simple and efficient CRISPR/Cas9-mediated homology directed repair platform for *Drosophila*

David L. Stern, Elizabeth Kim & Emily L. Behrman

Janelia Research Campus, Howard Hughes Medical Institute, Ashburn, VA, 20147 USA

Abstract

Homology-directed repair (HDR) is a powerful tool for modifying genomes in precise ways to address many biological questions. Use of Clustered Regularly Interspersed Short Palindromic Repeats (CRISPR)-Cas9 induced targeted DNA double-strand breakage has substantially simplified use of homology-directed repair to introduce specific perturbations in *Drosophila*, but existing platforms for CRISPR-Cas9-mediated HDR in *Drosophila* involve multiple cloning steps and have low efficiency. To simplify cloning of HDR plasmids, we designed a new plasmid platform, the Janelia Atalanta (pJAT) series, that exploits recent advances in dsDNA synthesis to facilitate Gateway cloning of gRNA sequences and homology arms in one step. Surprisingly, the pJAT plasmids yielded considerably higher HDR efficiency (approximately 25%) than we have observed with other approaches. pJAT plasmids work in multiple *Drosophila* species and exhibited such high efficiency that previously impossible experiments in *Drosophila*, such as driving targeted chromosomal inversions, were made possible. We provide pJAT plasmids for a range of commonly performed experiments including targeted insertional mutagenesis, insertion of phiC31-mediated attP landing sites, generation of strains carrying a germ-line source of Cas9, and induction of chromosomal rearrangements. We also provide “empty” pJAT plasmids with multiple cloning sites to simplify construction of plasmids with new functionality. The pJAT platform is generic and may facilitate improved efficiency CRISPR-Cas9 HDR in a wide range of model and non-model organisms.

Introduction

CRISPR-Cas9 induced mutagenesis has revolutionized experimental approaches in model and non-model organisms. DNA cuts induced by Cas9 or other enzymes[1,2] can be repaired by the non-homologous end-joining pathway to induce small deletions or cuts may be repaired by HDR if a homologous DNA template is present[3]. HDR provides the greatest power to manipulate gene function and to introduce new reagents into the germ line of experimental organisms, but CRISPR-Cas9 induced HDR works at low efficiency in many species.

HDR is normally implemented by introduction of three separate elements: Cas9 (or analogous enzyme), guide RNA, and homologous DNA. Usually, these three reagents are introduced as distinct components. In the most efficient systems, a source of gRNA and the homology arms are typically cloned into separate plasmids. Usually, plasmids containing homology arms are constructed by polymerase chain reaction (PCR) of homology arms from genomic DNA followed by cloning of arms together, often with a "payload" located between flanking homology arms. Generation of homology arms with PCR can be difficult for some target regions and cloning the homology arms with the payload also may have low efficiency, particularly when attempting to assemble multiple fragments.

We designed a new series of plasmids to simplify cloning for CRISPR-HDR experiments. The plasmid design includes two Gateway cloning sites for simultaneous introduction of long dsDNA fragments produced using new cost-effective DNA synthesis methods (Figure 1). The synthesized fragments incorporate homology arms between the *attL* Gateway cloning sites and one or both fragments includes a tRNA-sgRNA-tRNA array. We found that plasmids containing multiple copies of the standard Gateway negative selection marker, *ccdB*, were unstable[4] and we therefore introduced a novel dual selection system to ensure efficient simultaneous cloning of two attL cassettes. We placed a U6 promoter sequence flanking one or both Gateway cloning sites to drive transcription of the tRNA-sgRNA-tRNA array, followed by a U6 terminator; this combination provides efficient precise release of sgRNA molecules[5]. Any payload can then be placed between the Gateway cloning sites, and we have generated a series of plasmids carrying some commonly used payloads.

While we designed this plasmid for efficient cloning, we found that the plasmids yielded far higher HDR integration efficiencies on average than has been observed by us and others using other methods[3,6,7]. We have therefore named these plasmids the Janelia Atalanta (pJAT) series, after the mythological Greek heroine and exceptional archer (Supplementary Figure 1). The high efficiency of HDR with pJAT plasmids inspired us to attempt new kinds of experiments that have so far not been feasible in *Drosophila*, including introduction of chromosomal inversions.

The pJAT plasmids are modular and generic. One or two U6 promoter from any species can be introduced outside the Gateway cloning cassettes and any payload can be introduced between the cloning cassettes. pJAT plasmids may therefore be of value for HDR experiments in many model and non-model organisms.

Results

The pJAT *series dual-Gateway cloning platform*

Our initial aim was to build a plasmid platform that could utilize recent advances in DNA synthesis technology to simplify the cloning of reagents for CRISPR-Cas9 induced HDR. We found that some companies could synthesize long dsDNA fragments containing repetitive DNA attL sequences at the ends at a reasonable price (for example, 7 cents per bp from Twist Bioscience). This inspired us to design a dual-Gateway cloning platform for direct cloning of two fragments that each contain a homology arm (Gateway Cassettes 1 and 2; Figure 1A-C). To further reduce the number of plasmids that were required for experiments, we incorporated a tRNA-gRNA-tRNA design[5] directly into the synthesized fragments (Figure 1B, D). Our initial attempts at building a dual-Gateway plasmid followed earlier examples and simply duplicated the standard *ccdB* negative selection gene in two separate attR-attR cassettes[8]. We found, however, that every plasmid recovered during cloning carried a mutation in one of the *ccdB* genes, suggesting that high *ccdB* dosage is deleterious to *E. coli*[4]. We therefore replaced one of

84 the *ccdB* genes with a *sacB* gene, which allows negative selection by growing *E. coli* on plates
85 containing high levels of sucrose[9].
86 The pJAT plasmids contain one or two U6 promoters flanking the Gateway cloning
87 cassettes or restriction sites that can be used to introduce new U6 promoters. We have
88 generated pJAT plasmids containing multiple kinds of payloads, including (1) a germline source
89 of Cas9, (2) attP landing sites, (3) marker genes, and (4) a split-GFP system to report on
90 simultaneous HDR of two plasmids (Figure 2). All of the current pJAT plasmids utilize
91 fluorescent reporter genes expressed in different anatomical regions[10], which allow
92 recombination of multiple reagents into a single wild-type fly without the use of balancer
93 chromosomes. To facilitate introduction of novel payloads, we have generated one pJAT
94 plasmid that contains a multiple cloning site for both standard ligation based cloning and
95 Golden Gate cloning with BsaI or BbsI sites (Figure 2).
96 For plasmid construction, homology arms were synthesized by Twist Bioscience with
97 compatible attL sites and the company's adaptor sequences are left on for three reasons: (1)
98 synthesis sometimes fails without the adaptor sequences, probably because the repetitive attL
99 sites are then located at the ends of the synthesized fragments, (2) keeping adaptors reduces
100 synthesis cost; and (3) the adaptor sequences do not conflict with Gateway cloning. Synthesis of
101 arms confers many benefits compared with PCR based construction of HDR plasmids, including
102 the ability to include exogenous sequences, such as the tRNA-gRNA-tRNA array and other
103 elements, as described further below, and the ability to introduce single base pair
104 modifications. Synthesis by Twist Biosciences currently faces several limitations: (1) short
105 homology arms are difficult to synthesize, probably because the repetitive attL sites are then
106 positioned too close together; (2) the sequence cannot include more than 10 consecutive bp of
107 the same nucleotide; (3) there are limitations on regions containing strong AT/GC bias and on
108 repetitive sequences, which has prevented inclusion of multiple sgRNAs in a single synthesized
109 fragment. Some of these synthesis challenges can be overcome by introducing innocuous point
110 mutations, since HDR appears to be robust to considerable sequence variation relative to the
111 target sequence. Cloning into pJAT plasmids requires standard Gateway cloning reagents and

112 little hands-on time. A full protocol describing design of homology arms and all steps of cloning
113 is provided at protocols.io.
114
115 pJAT *plasmids yield high efficiency HDR*
116
117 Our initial experiments with pJAT plasmids yielded efficiencies of HDR of approximately
118 40-50%. We had previously only rarely observed such high efficiencies of HDR in *Drosophila* and
119 so we systematically targeted many loci in *D. melanogaster* and found that we could
120 successfully target all loci. We confirmed that all HDR products were integrated into the correct
121 locations using TagMap[11] with pJAT-specific primers (Materials and Methods). The average
122 integration efficiency—that is, the fraction of fertile G0 injected eggs that yielded at least one
123 positive event in the next generation—was approximately 25% for insertions into genes in
124 which null mutations are homozygous viable and was more variable and lower on average for
125 genes in which null mutations were homozygous lethal (Figure 3).
126 Seven of the injections into lethal genes (shown as separate data points in Figure 3)
127 yielded no events, but these were repeated injections using into only two loci. Despite these
128 failures, other injections into these two loci yielded some events, though at low frequency.
129 Thus, all genes were targetable with pJAT plasmids, but a few genes, and specifically a subset of
130 those that are homozygous lethal, showed low efficiency. This low efficiency did not appear to
131 result from the specific gRNA sequences used (data not shown) or the homology arm lengths
132 (Supplementary Table 1). One possibility, which requires further investigation, is that the high
133 efficiency of pJAT plasmids may induce homozygous null genotypes in many cells of the
134 developing embryo, leading to lethality or sterility.
135
136 *Multiple features contribute to high efficiency of* pJAT *plasmids*
137
138 To determine possible reasons for the high efficiency of HDR with pJAT plasmids, we
139 systematically varied sections of the synthesized fragments. We identified two features that
140 improved HDR efficiency. First, as has been documented previously[5], flanking the sgRNA with

141 tRNAs increased efficiency over co-injection with a sgRNA (Supplementary Figure 2).
142 Surprisingly, a pJAT plasmid containing the sgRNA, but no flanking tRNAs, had similar efficiency
143 to co-injecting with prepared sgRNA (Supplementary Figure 2), indicating that Cas9 can utilize a
144 sgRNA even when it is embedded within flanking irrelevant RNA sequences, similar to results
145 observed by others[7]. Second, use of intact dsDNA plasmids yielded higher efficiency HDR than
146 plasmids that contained homology arms flanked by CRISPR-Cas9 cut sites (Supplementary
147 Figure 3), which should linearize the plasmid DNA *in vivo* and which has been recommended
148 previously[12]. It is possible that the relatively long homology arms used here improved
149 efficiency, but we found that arms as short as 250 bp yielded similar efficiency as longer arms
150 (Supplementary Table 1). We did not test shorter arms, since it is challenging to synthesize
151 short arms with the long repeated attR sequences on both ends. The concentration of sgRNA
152 produced from a single U6 promoter does not appear to be limiting, since synthesis of the same
153 gRNA from two U6 promoters did not increase HDR efficiency (Supplementary Figure 4).
154 While pJAT plasmids provide sufficient gRNA for efficient HDR, we hypothesized that the
155 quantity of Cas9 protein may be limiting when Cas9 is introduced exogenously, either as mRNA
156 or protein. To test this idea, we built a pJAT plasmid that drives expression of a *Drosophila*
157 codon optimized Cas9 mRNA from a germline specific *nanos* promoter with a *nanos* 3'UTR to
158 localize Cas9 mRNA to the developing oocytes (Figure 2) and found that it increased HDR
159 efficiency approximately 2-3 fold compared to co-injection with *Cas9* mRNA (Supplementary
160 Table 2).
161 All of the experiments described above were performed by incubating injected embryos
162 at 22°C after injection. Given the known temperature sensitivity of Cas9[13], we performed a
163 small test of incubation temperature by placing eggs at either 20°C, 22°C, or 25°C for 4 h after
164 injection. We observed an increase in integration efficiency at higher temperatures
165 (Supplementary Table 3), suggesting that the effect of temperature on CRISPR-Cas9 HDR in
166 *Drosophila* should be investigated further.
167 Note that the efficiencies reported for many experiments shown in Figure 3 resulted
168 from injections using Cas9 mRNA and with incubation at 22°C, which we now know are sub-
169 optimal conditions. Thus, the average efficiencies reported here may underestimate the

average efficiency using optimal conditions. The availability of a high-efficiency CRISPR-HDR platform that works in multiple species invites new kinds of experiments. We next illustrate two kinds of experiments that have been challenging to implement with previous technology.

Scarless mutagenesis with pJAT *plasmids*

The use of synthesized homology arms and Gateway cloning can simplify the performance of scarless mutagenesis. One approach, which we have not explored, would be to insert a selectable marker at a target genome location and then, in a second set of injections, to replace the selectable marker with the intended genomic changes[14]. A second approach, which we illustrate here, is to place a selectable fluorescent marker between *piggyBac* transposon arms, which are included in the synthesized DNA fragments adjacent to homology arms that include the intended genomic changes[15]. In cases where the synthesized homology arms carry sites that differ from the genomic target, we have found that variable lengths of the synthesized homology arms, starting from the sites closest to the CRISPR cut site, are integrated into the genome. It is therefore best to place the intended genomic changes close to the *pBac* arms and to sequence the target region in HDR integrants to identify flies that carry the intended changes. The selectable marker, together with the *piggyBac* arms, is then removed by crossing flies to a strain expressing the *piggyBac* transposase gene (Figure 4). In the experiment performed here, we observed 58% integration efficiency (7 of 12 fertile injected G0 yielded integrants) into a site in *D. yakuba* and the *pBac* sequence was efficiently removed from multiple lines. This approach allowed efficient recovery of two scarless individual nucleotide changes at the targeted locus (Supplementary Figure 5).

pJAT *plasmids can direct one-step targeted chromosomal inversions*

The HDR efficiency of pJAT plasmids was considerably higher than we have observed using other approaches and this high efficiency emboldened us to try more complex experiments. One experiment that would be of considerable value, especially for studies of

199 non-*melanogaster Drosophila* species, would be the ability to generate chromosomal inversions
200 that could subsequently be used to balance deleterious alleles[16]. This experiment requires
201 efficient cutting at two chromosomal sites followed by inversion of the intervening sequence
202 (Figure 5A). To encourage production of the inversion event, we designed a pair of pJAT
203 plasmids where each plasmid carried homology arms oriented in the same direction as the
204 intended inverted chromosomal region (Figure 5B). To simplify detection of simultaneous
205 integration of both plasmids, potentially indicative of an inversion, we built three pairs of pJAT
206 plasmids expressing split-GFP in either the eyes, the thorax, or the abdomen (Figure 2).
207 We targeted three inversions of approximately 58 kb to 3 Mbp in *Drosophila yakuba* to
208 provide potential balancer chromosomes for reagents that we had previously built at the
209 *fruitless* and *doublesex* genes in this species (Figure 5c). We targeted breaks within genes that
210 are expected to be homozygous deleterious or lethal. We detected multiple events for each
211 targeted inversion, at efficiencies of 8-23% (Supplementary Table 4).
212 We PCR amplified fragments corresponding to the expected inversion event breakpoints
213 (Supplementary Figure 6) and confirmed that the sequences of both breakpoints were oriented
214 as expected (Supplementary Figure 7). We crossed the three *D. yakuba* inversions to null alleles
215 of either *dsx* or *fru*, which they were designed to balance, and found that they all balanced the
216 targeted alleles for multiple generations. Thus, single inversions can be quickly introduced to
217 balance specific alleles in *Drosophila* species. This technology will substantially simplify the
218 maintenance of transgenic reagents and mutants in non-*melanogaster Drosophila* species. It is
219 possible that multiple inversions can be introduced serially onto a single chromosome arm to
220 generate balancer chromosomes of even greater utility[10], and we provide three sets of split-
221 GFP reagents that may enable these experiments (Figure 2).
222
223 **Discussion**
224
225 We have developed a series of new plasmids that provide a simple cloning platform and
226 enable high efficiency HDR in multiple *Drosophila* species. The plasmid design is flexible and
227 allows introduction of any payload of interest. The efficiency of pJAT plasmids is so high that it

228 is almost certainly preferable to random integration via transposable elements for most
229 purposes and may even be more efficient than the most widely used method of transgenesis in
230 *Drosophila* at the moment, site-specific recombination into attP sites[17]. We have reported
231 previously that some strains and some species appear to be resistant to specific transposable
232 elements and to *attP-attB* integration[18]. In fact, we previously tried multiple times to introduce
233 a *nos-Cas9* transgene using transposable elements into the specific *D. simulans* strain used in
234 this study without success, but we identified multiple independent events with a single
235 injection of a pJAT plasmid carrying *nos-Cas9*. Thus, pJAT plasmids are probably a preferable
236 method of transgenesis to random integration using transposable elements, especially for
237 studies of non-*melanogaster Drosophila* species.

238 We designed the pJAT plasmids for ease of cloning using synthesized homology arms
239 that incorporate tRNA-sgRNA-tRNA arrays. Because these arms are synthesized, any
240 modifications to the native sequence can be introduced during synthesis and then integrated
241 into the genome. We illustrated the power of this approach by including mobilization
242 sequences of the *piggyBac* transposon into the synthesized arms. This allows efficient scarless
243 removal of the transposon and reporter gene, leaving behind substitutions introduced into the
244 genome (Figure 4). An additional illustration of the utility of this approach is that additional
245 CRISPR target sites can be introduced flanking the homology arms, allowing the homology arms
246 and payload to be linearized *in vivo* (Supplementary Figure 3). This does not appear to increase
247 HDR efficiency using pJAT plasmids in *Drosophila* (Supplementary Figure 3), which is consistent
248 with reports of HDR induced by zinc-finger nucleases in *Drosophila* that showed that circular
249 donor DNA was more efficient than linearized DNA[2]. However, linearization may increase
250 efficiency of HDR or of homology-mediated end joining in other systems[19,20].

251 We initially attempted to build the double-Gateway system using multiple *ccdB*
252 containing cassettes, as has been demonstrated by others[8]. However, we discovered during
253 subsequent cloning that in every case one of the two *ccdB* genes had been inactivated. This
254 may result from the dosage sensitivity of *E. coli* to *ccdB* copy number[4]. We therefore developed
255 a novel Gateway-like second cloning cassette that exploits the well-established strong negative
256 selective capability of the *SacB* gene[21]. When *E. coli* are grown on high levels of sucrose,

257 expression of the *SacB* gene causes lethality. Thus, this stabilized double-Gateway system
258 dramatically improved cloning efficiency of two synthesized fragments containing
259 complementary *attL* sites over a design that utilizes two cassettes both using the *ccdB* gene.
260 While we designed the Janelia Atalanta series to simplify cloning, we found that these
261 plasmids also increased HDR efficiency compared with other methods that we have tested and
262 that have been reported. Often, HDR in many genes fails[3,6] and, when it succeeds and has been
263 reported efficiency is approximately 1-10% on average. Although difficult to quantify,
264 publication bias may mean these reported efficiencies are over-estimates of true efficiencies,
265 since we are aware of multiple examples of failed CRISPR-HDR attempts in *Drosophila* species
266 performed by other research groups. We so far have been able to target every locus attempted
267 and on average targeting genes or genomic regions that have non-lethal mutant phenotypes
268 results in approximately 25% of fertile injected animals yielding correct insertion events. We
269 performed a series of experiments to try to determine what might contribute to this increased
270 efficiency and it appears that multiple factors contribute to higher efficiency HDR. Some of the
271 most important factors appear to be (1) production of sgRNA from a tRNA-sgRNA-tRNA array,
272 (2) injection into embryos with a germline source of Cas9 protein, (3) homology arms of at least
273 250 bp long, (4) circular plasmid DNA, and possibly (5) increasing the incubation temperature to
274 25°C for a time after injection.
275 Despite the overall high efficiency of HDR with pJAT plasmids, we identified a strikingly
276 lower efficiency on average with plasmids targeting genes with lethal null phenotypes. A subset
277 of these "lethal" genes did show high efficiencies, however. In limited experiments, we found
278 no evidence that lower HDR efficiencies resulted from the specific gRNA or homology arms
279 used, but we cannot rule out the possibility that these variables influenced efficiency. One
280 possibility which we have not tested is that the pJAT plasmids are so efficient that when the
281 reagents work at one targeted allele in an individual, the second allele is also hit at high
282 frequency. This would cause injected animals to be mosaic for homozygous null mutations,
283 which may lead to lethality of sterility of many flies carrying HDR events.
284 The most powerful demonstration of the high efficiency of pJAT plasmids is that they
285 could be used to introduce two simultaneous breaks in a single chromosome and facilitate

286 inversion of large chromosomal regions through HDR (Figure 5, Supplementary Figures 5 & 6).
287 Three independent experiments, using two separate injection companies, yielded inversions
288 (Supplementary Table 4). These inversions provide practical benefits, since they can be used to
289 balance deleterious alleles and will simplify stock maintenance. It may also be possible to use
290 pJAT plasmids to generate multiply inverted balancer chromosomes with wide applicability[16]. It
291 has not escaped our attention that this approach may also allow reversion of naturally
292 occurring chromosomal inversions[22], which often become hot-spots of evolutionary
293 divergence[23]. Such experiments may allow, for the first time, detailed recombination-based
294 identification of loci "locked" within non-recombining inversions that have contributed to
295 phenotypic divergence.
296 The pJAT plasmids were designed to provide a generic platform for introducing many
297 variant elements easily and it is possible that pJAT plasmids may provide an improved CRISPR-
298 HDR platform for other species. One potentially species-specific component of this first set of
299 pJAT plasmids are the U6 promoters. We used the *D. melanogaster* U6-3 promoter for all of the
300 experiments described in this paper and we observed similar HDR efficiencies in *D.*
301 *melanogaster*, *D. simulans*, and *D. yakuba* (Figure 3), suggesting that this U6-3 promoter works
302 well for these species. This U6 promoter could be easily swapped with a different species-
303 specific or inducible promoter. We have therefore generated pJAT77, where cloning sites can
304 allow any promoter to be placed on either or both sides of the Gateway cloning cassettes.
305 Some pJAT plasmids presented in this paper (Figure 2_ contain other species-specific
306 components that may not work efficiently in other species. For example, some of these
307 plasmids include germ-line specific promoters and 3'UTRs that were derived from the *D.*
308 *melanogaster nanos* and *vasa* genes. It is possible that these will not work efficiently in other
309 species. But the pJAT plasmids with multiple cloning sites allow efficient cloning of new
310 payloads with other species-specific components. It will be interesting to determine whether
311 pJAT plasmids increase HDR efficiency in organisms other than *Drosophila*.
312
313 **Methods**
314

315 *Construction of Janelia Atalanta (*pJAT*) plasmids*

316

317 pJAT plasmids were assembled by Golden Gate cloning[24] of PCR amplified and
318 synthesized fragments. All plasmids reported here are available from Addgene under plasmid
319 numbers 204289-204312.

320 Gateway compatible homology arms were synthesized by Twist Bioscience with
321 Adaptors On. Because these sequences contain almost identical attL sites at either end,
322 synthesis is inefficient and often fails with Adaptors Off. In addition, since these fragments are
323 cloned into the pJAT plasmids using Golden Gate cloning, there is no need to remove the Twist
324 synthesis adaptors. Golden Gate cloning was performed as follows.

325

326 pJAT plasmid (~50 ng/uL)	1 uL
327 Homology arm left (50 ng/uL)	0.5 uL
328 Homology arm right(50 ng/uL)	0.5 uL
329 LR Clonase II	0.25 uL

330

331 Reaction was incubated at 25°C in a thermocycler for 2-12 hours. Then 0.125 uL of
332 Proteinase K (provided with LR clonase kit) was added and sample was incubated in a
333 thermocycler at 37°C for 20 minutes. The entire reaction volume was gently mixed with at least
334 25 uL of Zymo Mix&Go Competent Cells thawed on ice. The mixture was incubated for 30
335 minutes on ice, heat shocked for 30 seconds at 42°C, and returned to ice. 100 uL of SOC was
336 added and the mixture was shaken at 200 RPM at 37°C for 1 hour. The entire mixture was
337 plated on Tryptone-Yeast + Sucrose plates + Spectinomycin plates. The entire protocol,
338 including a guide for designing and ordering homology arms, is provided at Protocols.io:
339 dx.doi.org/10.17504/protocols.io.bp2l6bjokgqe/v1.

340

341 *Injection of* Drosophila *embryos*

342

343 Most pJAT plasmids were injected into Drosophila embryos by Rainbow Transgenics and
344 some were injected by Genetivision. Initially, plasmids were co-injected with Cas9 RNA
345 generated by *in vitro* transcription from plasmid encoding Cas9[10]. After we generated fly lines
346 carrying a *nanos-Cas9* transgene (*pJAT17*), plasmids were injected into flies homozygous for
347 *pJAT17* and fertile adults emerging from injected eggs were outcrossed to a wild-type strain
348 and offspring were screened for fluorescent reporter genes. The genomic insertion location of
349 all integrants were determined using TagMap[11] with the following TagMap PCR primers, where
350 the underlined sequence represents the Tn5 MEB adaptor and the non-underlined sequence
351 represents the sequence specific to each pJAT plasmid.
352

Primer	Sequence
Tn5 ME B adaptor-attB4	GTCTCGTGGGCTCGGAGATGTGTATAAGAGACAGAGCTGGACAACTTTGTATAGAAAAG
Tn5 ME B adaptor-P767_attB5	GTCTCGTGGGCTCGGAGATGTGTATAAGAGACAGCGTCTCACAACTTTGTATACAAAAG
Tn5 ME B adaptor-P776_attB5	GTCTCGTGGGCTCGGAGATGTGTATAAGAGACAGCGAGTATAATCAACTTTGTATACAAAAG
Tn5 ME B adaptor-P777_attB5	GTCTCGTGGGCTCGGAGATGTGTATAAGAGACAGAAGCAACCCAACTTTGTATACAAAAG
Tn5 ME B adaptor-P795_attB5	GTCTCGTGGGCTCGGAGATGTGTATAAGAGACAGAACAACTAGTCAACTTTGTATACAAAAG
Tn5 ME B adaptor-P832_attB5	GTCTCGTGGGCTCGGAGATGTGTATAAGAGACAGCTCTCTAGTCAACTTTGTATACAAAAG
Tn5 ME B adaptor-P859_attB5	GTCTCGTGGGCTCGGAGATGTGTATAAGAGACAGCTCACCATCAACTTTGTATACAAAAG
Tn5 ME B adaptor-P887_attB5	GTCTCGTGGGCTCGGAGATGTGTATAAGAGACAGCTCGGCAACTTTGTATACAAAAG

353

354 *Design and generation of scarless site specific mutations*

355

356 Gateway compatible fragments were designed to include the 5' and 3' pBac sequences
357 required for transposition internal to the targeting homology arms (Figure 4). Fragments were
358 synthesized by Twist Biosciences and Gateway cloned into pJAT10 as described above.

359

360 *Design and generation of targeted inversions*

361

362 Gateway compatible fragments were designed with homology arms configured to
363 promote chromosomal inversions (Figure 5). Fragments were synthesized by Twist Biosciences

and Gateway cloned into pJAT21 and pJAT25 as described above. Both plasmids were injected simultaneously into flies carrying a nos-Cas9 transgene.

Acknowledgements

We thank Carlos Machado, Thomas Ravenscroft, and Gerry Rubin for helpful comments on the manuscript. Elements of Figures 1, 4, and 5 and Supplementary Figures 2, 3, and 4 were created with BioRender.com. We especially thank Justine Ayelet Stern for designing and creating Supplementary Figure 1 and for recommending the name Atalanta for these plasmids.

Author Contributions

D.L.S. conceptualized, designed, and constructed most of the plasmids and performed much of the fly work. E.K. assisted with construction and quality control of plasmids and with fly work. E.L.B. constructed pJAT17 and confirmed its utility. The paper was written by D.L.S. with input from E.K. and E.L.B.

Ethics Declarations

HHMI has filed a provisional patent, number 63/507,335, for the inventor D.L.S. covering vectors and methods for efficient cloning and homology directed repair.

385 **References**

386

387 1. Joung, J.K., and Sander, J.D. (2013). TALENs: a widely applicable technology for targeted
388 genome editing. Nat. Rev. Mol. Cell Biol. *14*, 49–55. 10.1038/nrm3486.

389 2. Beumer, K.J., Trautman, J.K., Bozas, A., Liu, J.L., Rutter, J., Gall, J.G., and Carroll, D. (2008).
390 Efficient gene targeting in Drosophila by direct embryo injection with zinc-finger nucleases.
391 Proc Natl Acad Sci U A *105*, 19821–19826. 10.1073/pnas.0810475105.

392 3. Gratz, S.J., Ukken, F.P., Rubinstein, C.D., Thiede, G., Donohue, L.K., Cummings, A.M., and
393 Oconnor-Giles, K.M. (2014). Highly specific and efficient CRISPR/Cas9-catalyzed homology-
394 directed repair in Drosophila. Genetics *196*, 961–971. 10.1534/genetics.113.160713.

395 4. Afif, H., Allali, N., Couturier, M., and Melderen, L.V. (2001). The ratio between CcdA and
396 CcdB modulates the transcriptional repression of the ccd poison–antidote system. Mol.
397 Microbiol. *41*, 73–82. https://doi.org/10.1046/j.1365-2958.2001.02492.x.

398 5. Port, F., and Bullock, S.L. (2016). Augmenting CRISPR applications in Drosophila with tRNA-
399 flanked sgRNAs. Nat. Methods *13*, 852–854. 10.1038/nmeth.3972.

400 6. Ding, Y., Berrocal, A., Morita, T., Longden, K.D.K.D., and Stern, D.L.D.L. (2016). Natural
401 courtship song variation caused by an intronic retroelement in an ion channel gene. Nature
402 *536*, 329–332. 10.1038/nature19093.

403 7. Kanca, O., Zirin, J., Hu, Y., Tepe, B., Dutta, D., Lin, W.-W., Ma, L., Ge, M., Zuo, Z., Liu, L.-P., et
404 al. (2022). An expanded toolkit for Drosophila gene tagging using synthesized homology
405 donor constructs for CRISPR-mediated homologous recombination. eLife *11*, e76077.
406 10.7554/eLife.76077.

407 8. Aboulela, M., Tanaka, Y., Nishimura, K., Mano, S., Kimura, T., and Nakagawa, T. (2017). A
408 dual-site gateway cloning system for simultaneous cloning of two genes for plant
409 transformation. Plasmid *92*, 1–11. 10.1016/j.plasmid.2017.05.001.

410 9. Li, X., Thomason, L.C., Sawitzke, J.A., Costantino, N., and Court, D.L. (2013). Positive and
411 negative selection using the tetA-sacB cassette: recombineering and P1 transduction in
412 Escherichia coli. Nucleic Acids Res. *41*, e204. 10.1093/nar/gkt1075.

413 10. Stern, D.L. (2022). Transgenic tools for targeted chromosome rearrangements allow
414 construction of balancer chromosomes in non- *melanogaster Drosophila* species. G3
415 GenesGenomesGenetics *12*, jkac030. 10.1093/g3journal/jkac030.

416 11. Stern, D.L. (2016). Tagmentation-Based Mapping (TagMap) of Mobile DNA Genomic
417 Insertion Sites. bioRxiv, 1–7. 10.1101/037762.

418 12. Kanca, O., Zirin, J., Garcia-Marques, J., Knight, S.M., Yang-Zhou, D., Amador, G., Chung, H.,
419 Zuo, Z., Ma, L., He, Y., et al. (2019). An efficient CRISPR-based strategy to insert small and
420 large fragments of DNA using short homology arms. eLife *8*, e51539. 10.7554/eLife.51539.

421 13. Xiang, G., Zhang, X., An, C., Cheng, C., and Wang, H. (2017). Temperature effect on CRISPR-
422 Cas9 mediated genome editing. J. Genet. Genomics *44*, 199–205.
423 10.1016/j.jgg.2017.03.004.

424 14. Lamb, A.M., Walker, E.A., and Wittkopp, P.J. (2016). Tools and strategies for scarless allele
425 replacement in Drosophila using CRISPR/Cas9. Fly (Austin) *0*, 1–12.
426 10.1080/19336934.2016.1220463.

427 15. Nyberg, K.G., and Carthew, R.W. (2022). CRISPR-/Cas9-Mediated Precise and Efficient
428 Genome Editing in Drosophila. Methods Mol. Biol. Clifton NJ *2540*, 135. 10.1007/978-1-
429 0716-2541-5_6.

430 16. Miller, D.E., Cook, K.R., and Hawley, R.S. (2019). The joy of balancers. PLoS Genet. *15*,
431 e1008421. 10.1371/journal.pgen.1008421.

432 17. Groth, A.C., Fish, M., Nusse, R., and Calos, M.P. (2004). Construction of Transgenic
433 Drosophila by Using the Site-Specific Integrase From Phage {phi}C31. Genetics *166*, 1775–
434 1782.

435 18. Stern, D.L., Crocker, J., Ding, Y., Frankel, N., Kappes, G., Kim, E., Kuzmickas, R., Lemire, A.,
436 Mast, J.D., and Picard, S. (2017). Genetic and Transgenic Reagents for Drosophila simulans,
437 D. mauritiana , D. yakuba , D. santomea, and D. virilis. G3, 1–10. 10.1534/g3.116.038885/-
438 /DC1.1.

439 19. Bai, H., Liu, L., An, K., Lu, X., Harrison, M., Zhao, Y., Yan, R., Lu, Z., Li, S., Lin, S., et al. (2020).
440 CRISPR/Cas9-mediated precise genome modification by a long ssDNA template in zebrafish.
441 BMC Genomics *21*, 67. 10.1186/s12864-020-6493-4.

442 20. Wierson, W.A., Welker, J.M., Almeida, M.P., Mann, C.M., Webster, D.A., Torrie, M.E., Weiss,
443 T.J., Kambakam, S., Vollbrecht, M.K., Lan, M., et al. (2020). Efficient targeted integration
444 directed by short homology in zebrafish and mammalian cells. eLife *9*, e53968.
445 10.7554/eLife.53968.

446 21. Reyrat, J.-M., Pelicic, V., Gicquel, B., and Rappuoli, R. (1998). Counterselectable Markers:
447 Untapped Tools for Bacterial Genetics and Pathogenesis. Infect. Immun. *66*, 4011–4017.
448 10.1128/IAI.66.9.4011-4017.1998.

449 22. Dobzhansky, T., and Sturtevant, A.H. (1937). Inversions in the chromosomes of Drosophila
450 pseudoobscura. Genetics *23*, 28–64.

451 23. Joron, M., Frezal, L., Jones, R.T., Chamberlain, N.L., Lee, S.F., Haag, C.R., Whibley, A.,
452 Becuwe, M., Baxter, S.W., Ferguson, L., et al. (2011). Chromosomal rearrangements

453 maintain a polymorphic supergene controlling butterfly mimicry. Nature *477*, 203–206.
454 10.1038/nature10341.

455 24. Engler, C., Kandzia, R., and Marillonnet, S. (2008). A One Pot, One Step, Precision Cloning
456 Method with High Throughput Capability. PLoS ONE *3*, e3647.
457 10.1371/journal.pone.0003647.

458

459 **Figure Legends**

460

461 Figure 1 – Design and use of the Janelia Atalanta plasmids. (A) Generic design of the Janelia
462 Atalanta series. Each plasmid contains two Gateway compatible cloning sites, flanked on the
463 left and right, respectively, by attR3-attR4 and attR5-attR6 sites. Each Gateway compatible
464 cassette contains a different positive and negative selection marker. The negative selection
465 markers *ccdB* and *SacB* can be selected simultaneously by cloning into *ccdB* sensitive cells and
466 plating on minimal media containing a high concentration of sucrose. Each Atalanta plasmid
467 contains one or two U6 promoters flanking the Gateway cassettes and a payload between the
468 Gateway cassettes. (B) DNA fragments or plasmids containing paired attL3-attL4 and attL5-attL6
469 sites can be cloned into the based Atalanta plasmid simultaneously. In this example, synthetic
470 DNA fragments containing left and right homology arms and a tRNA-sgRNA-tRNA array are
471 cloned into the Gateway sites. The plasmid thus provides a source both of sgRNA and of
472 homology arms for homology directed repair. (C) An example of an Atalanta plasmid after
473 cloning of Gateway-compatible arms that is ready for injection into *Drosophila* embryos. Cas9 is
474 provided either through co-injection of Cas9 mRNA or protein or by injection into embryos
475 expressing Cas9 in the germline. (D) Detail of the components of a generic tRNA-sgRNA-tRNA
476 region cloned downstream of the U6 promoter.

477

478 Figure 2 – Payloads of Janelia Atalanta plasmids. (A) A set of plasmids containing fluorescent
479 protein markers, attP sites, and removable fluorescent protein markers useful for targeted
480 mutagenesis and generation of attP landing sites. (B) Plasmids to facilitate cloning of novel
481 payloads. MCS=Multiple Cloning Site. (C) Plasmids carrying various effectors, including *nanos-*
482 *Cas9* (pJAT17), B3 integrase under heat shock control (pJAT 43), and two plasmids expressing
483 *vasa*-phiC31 integrase with different fluorescent protein markers (pJAT 56, pJAT 62). (D)
484 Plasmids carrying split-*GFP* constructs under three alternative promoter systems for
485 construction of chromosomal inversions.

486

487 Figure 3 – Integration efficiencies of Atalanta homology directed repair payloads into
488 *Drosophila* species. The percent of positive events is plotted against the number of viable
489 crosses screened. (A) Approximately 25% of injected animals producing fertile adults yielded
490 integration events into genes categorized as "viable" on Flybase or into non-genic regions. No
491 obvious difference was observed in integration efficiencies between the three *Drosophila*
492 species *D. melanogaster*, *D. simulans*, and *D. yakuba*. (B,) Integration efficiency for payloads
493 targeting genes categorized as "lethal" on Flybase (B).
494
495 Figure 4 – Schematic representation of scarless genome modification using pJAT plasmid. (A, B)
496 Diagram of a pJAT plasmid illustrating the location of the synthesized *pBac* transposon 5' and 3'
497 arms internal to the synthesized homology arms (A). The gRNA, included within the tRNA-gRNA-
498 tRNA array on the left homology arm, targets a genomic site that includes a TTAA motif (B), the
499 native target site for the *pBac* transposon. The synthesized right homology arm includes an
500 additional TTAA sequence between the 3' *pBac* sequence and the right homology arm.
501 Intended modifications to the genomic sequence can be included in either or both homology
502 arms. (C) Representation of the genomic sequence after integration of the pJAT plasmid. Flies
503 containing the intended genomic modification(s) can be identified by PCR and sequencing. (D)
504 After exposure to a source of *pBac* transposase, flies can be recovered that have lost the
505 reporter gene and contain the intended scarless genome modification.
506
507 Figure 5 – Design of pJAT plasmids for targeted inversions. (A) Schematic illustrating the
508 position and orientation of DNA sequences flanking two cut sites before (top) and after
509 (bottom) a chromosomal inversion. (B) Illustration of two pJAT plasmids, each containing one
510 half of a split-GFP reporter and a gRNA targeting one of the two intended cut sites. Each
511 plasmid includes synthesized arms oriented in the direction of the intended inversion so that
512 homology directed repair at both sites simultaneously will tend to drive an inversion. (C)
513 Illustration of three inversions targeted on the right arm of chromosome 3 in *D. yakuba*. The
514 positions of the *fruitless* (*fru*) and *Doublesex* (*dsx*) genes are shown in green. The locations of

515 target gRNA sites in the genes are shown in magenta. The three targeted inversions are shown
516 in beige.
517
518 Supplementary Figure Legends
519
520 Supplementary Figure 1 - Icon for the Janelia Atalanta series of plasmids. Representation of the
521 Greek goddess Atalanta practicing archery (artwork by Justine Ayelet Stern).
522
523
524 Supplementary Figure 2 - Effect of tRNA-sgRNA-tRNA array on CRISPR-Cas9 HDR efficiency.
525 Three plasmids were created where the left homology arm contained either no tRNA and
526 sgRNA (A), just the sgRNA (B), or the full tRNA-sgRNA-tRNA array (C). Injections of the plasmid
527 without a sgRNA were supplemented with *in vitro* transcribed sgRNA. All plasmids targeted the
528 *CG42402* gene. The table shows the HDR efficiency for each construct type.
529
530 Supplementary Figure 3 – To test the hypothesis that *in vivo* linearization of the template DNA
531 increases the efficiency of HDR, plasmids targeting two loci were constructed either without (A)
532 or with (B) CRISPR target sites for the sgRNA encoded in the tRNA-sgRNA-tRNA array. Results
533 are shown in the table, which illustrates that plasmids containing the flanking CRISPR sites did
534 not increase HDR efficiency for two genes.
535
536 Supplementary Figure 4 – To test the hypothesis that sgRNA concentration limited HDR,
537 plasmids including either one (A) or two (B) sources of sgRNA were constructed. Results are
538 shown in the table, which illustrates that plasmids containing two sources of sgRNA did not
539 increase HDR efficiency for two genes on average.
540
541 Supplementary Figure 5 – Sequence confirmation of scarless genome mutagenesis. (A)
542 Sequencing of genomic DNA containing inserted pBac transposable element with internal MHC-
543 DsRed reporter. Left homology arm includes intended 2 bp changes. PCR fragments were

544 generated with primers external to homology arms (green) and internal to the pBac transposon
545 and Sanger sequenced with internal primers (magenta). Sanger sequencing products were
546 aligned to the original genome sequence and mismatches are shown in the Identity track and
547 below the Sanger sequencing read. (B) A PCR product of the final scarless allele generated with
548 primers shown (green) was Nanopore sequenced and aligned to the original genome sequence
549 and mismatches are shown in the Identity track and within the consensus Nanopore sequencing
550 read.
551
552 Supplementary Figure 6 – Detailed maps from the *D. yakuba* genome of the gRNA sites
553 (magenta), homology arms (yellow), intended inversion ends (brown), and PCR primers for the
554 genes *VMS100-2* (A), *fray* (B), *Os-C* (C), and *Ids* (D).
555
556 Supplementary Figure 7 – Sequences of PCR products generated using primers illustrated in
557 Supplementary Figure 6 on strains carrying the putative inversions. Three inversions were
558 generated, one between *VMS100-2* and *fray* (A, B), one between *Osc* and *Ids* (C, D), and one
559 between *VMS100-2* and *Ids* (E, F).
560

Figure 1

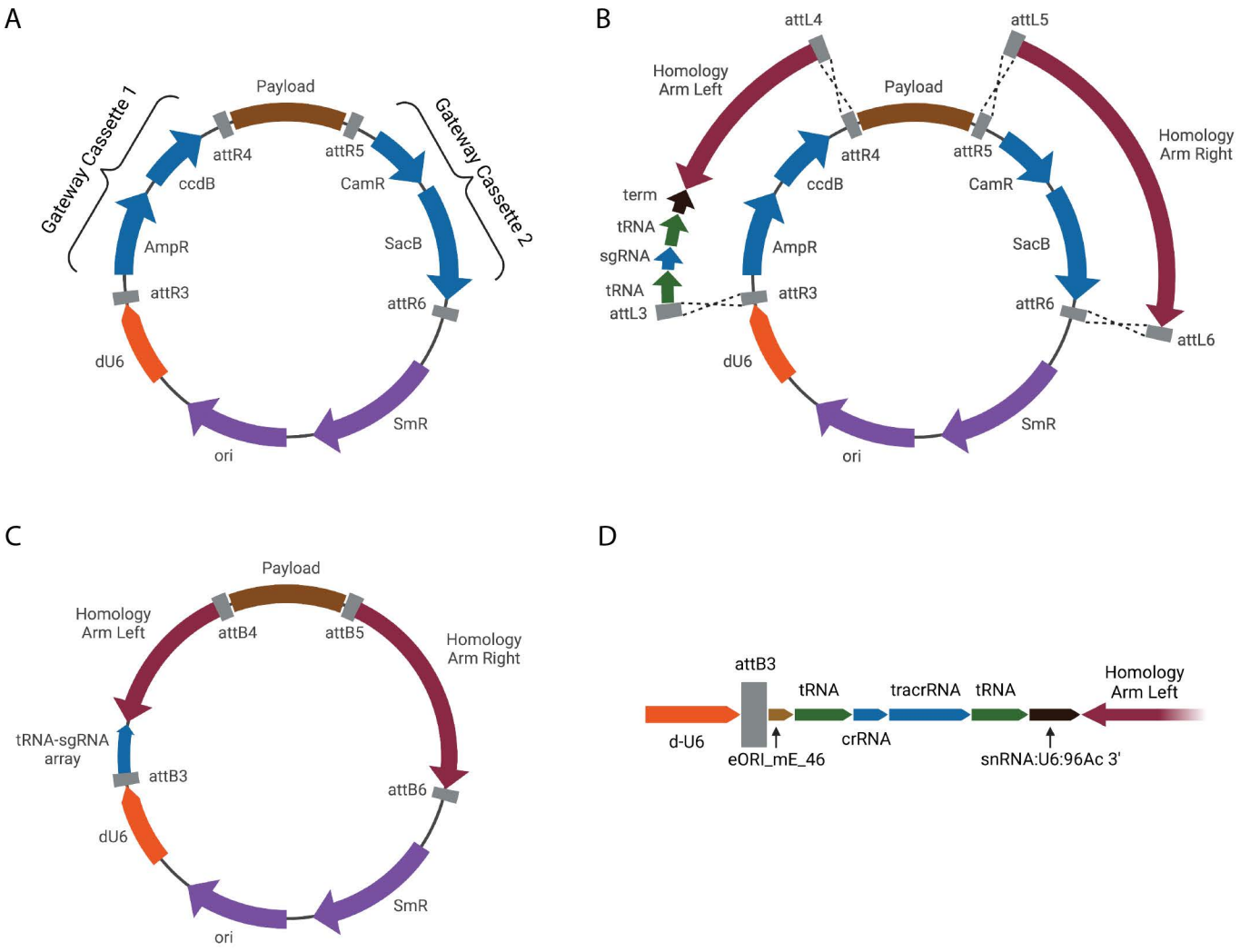
A
Gateway Cassette 1
Gateway Cassette 2
Payload
attR4
attR5
ccdB
CamR
AmpR
SacB
attR3
attR6
dU6
SmR
ori
B
attL4
attL5
Homology Arm Left
Payload
Homology Arm Right
attR4
attR5
ccdB
CamR
term
tRNA
sgRNA
tRNA
attL3
AmpR
SacB
attR3
attR6
attL6
dU6
SmR
ori
C
Payload
Homology Arm Left
attB4
attB5
Homology Arm Right
tRNA-sgRNA array
attB3
attB6
dU6
SmR
ori
D
attB3
tRNA
tracrRNA
tRNA
Homology Arm Left
d-U6
eORI_mE_46
crRNA
snRNA:U6:96Ac 3'

Figure 2

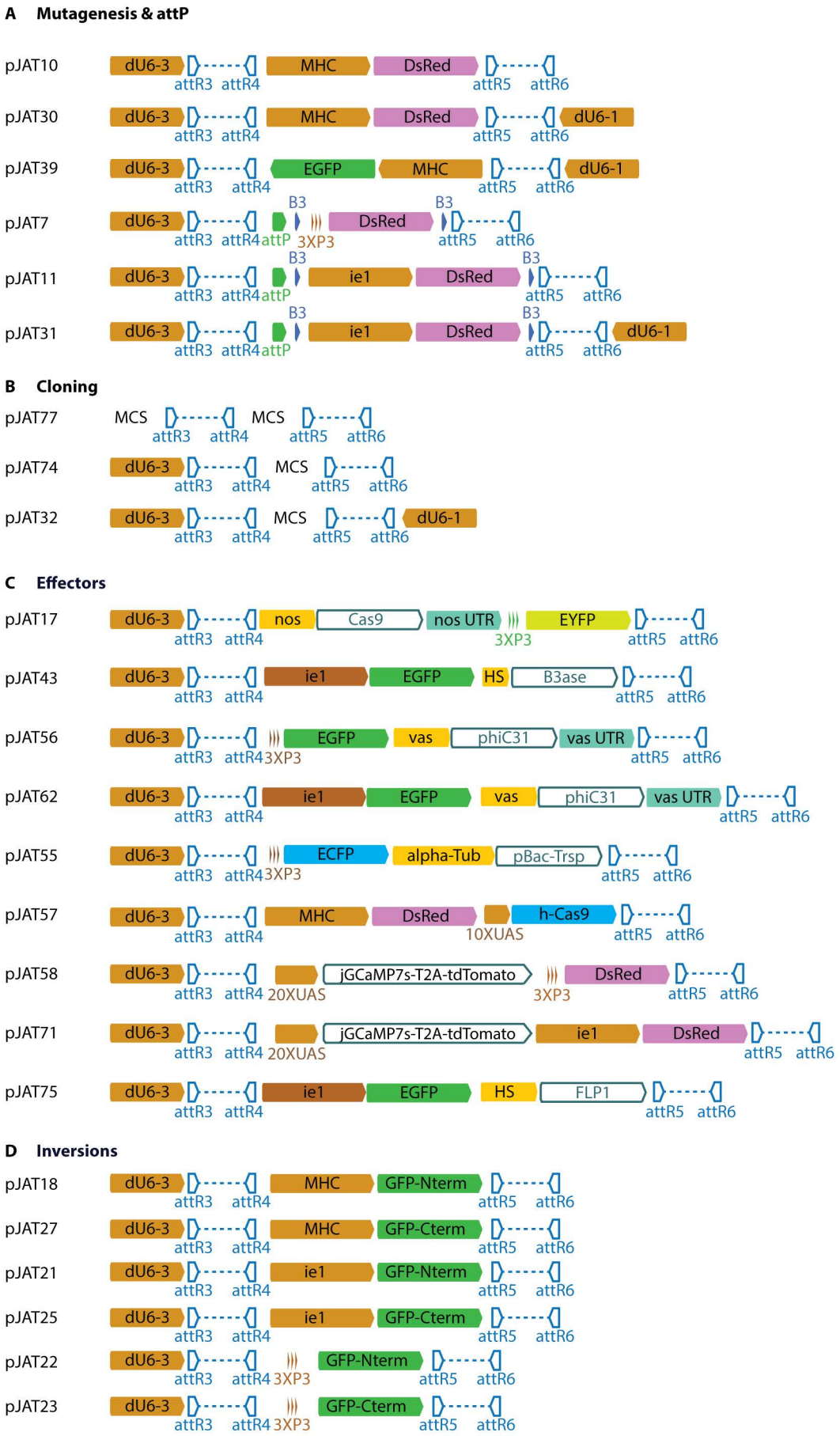
A Mutagenesis & attP
pJAT10
dU6-3
attR3 attR4
MHC
DsRed
attR5 attR6
pJAT30
dU6-1
pJAT39
EGFP
pJAT7
B3
attP
3XP3
pJAT11
ie1
pJAT31
B C D
MCS
pJAT74
pJAT32
pJAT17
nos
Cas9
nos UTR
EYFP
pJAT43
HS
B3ase
pJAT56
vas
phiC31
vas UTR
pJAT62
pJAT55
ECFP
alpha-Tub
pBac-Trsp
pJAT57
h-Cas9
10XUAS
pJAT58
jGCaMP7s-T2A-tdTomato
20XUAS
pJAT71
pJAT75
FLP1
pJAT18
GFP-Nterm
pJAT27
GFP-Cterm
pJAT21
pJAT25
pJAT22
pJAT23

Figure 3

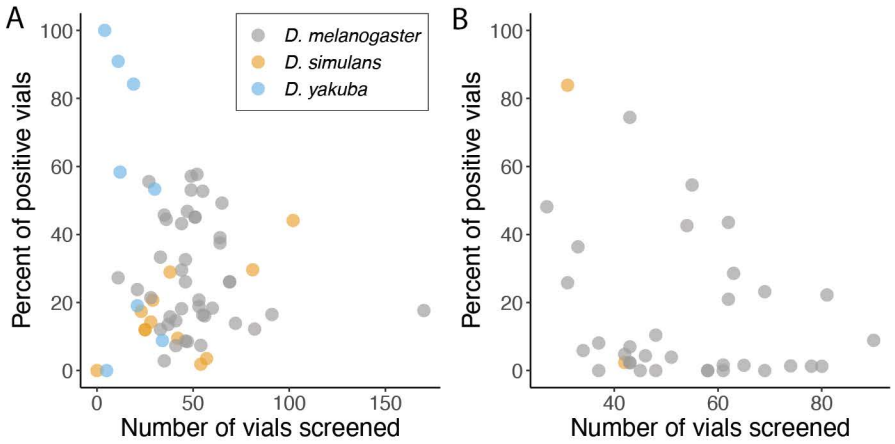
A
B
D. melanogaster
D. simulans
D. yakuba
Percent of positive vials
Number of vials screened
0
20
40
60
80
100
0
50
100
150
40
60
80

Figure 4

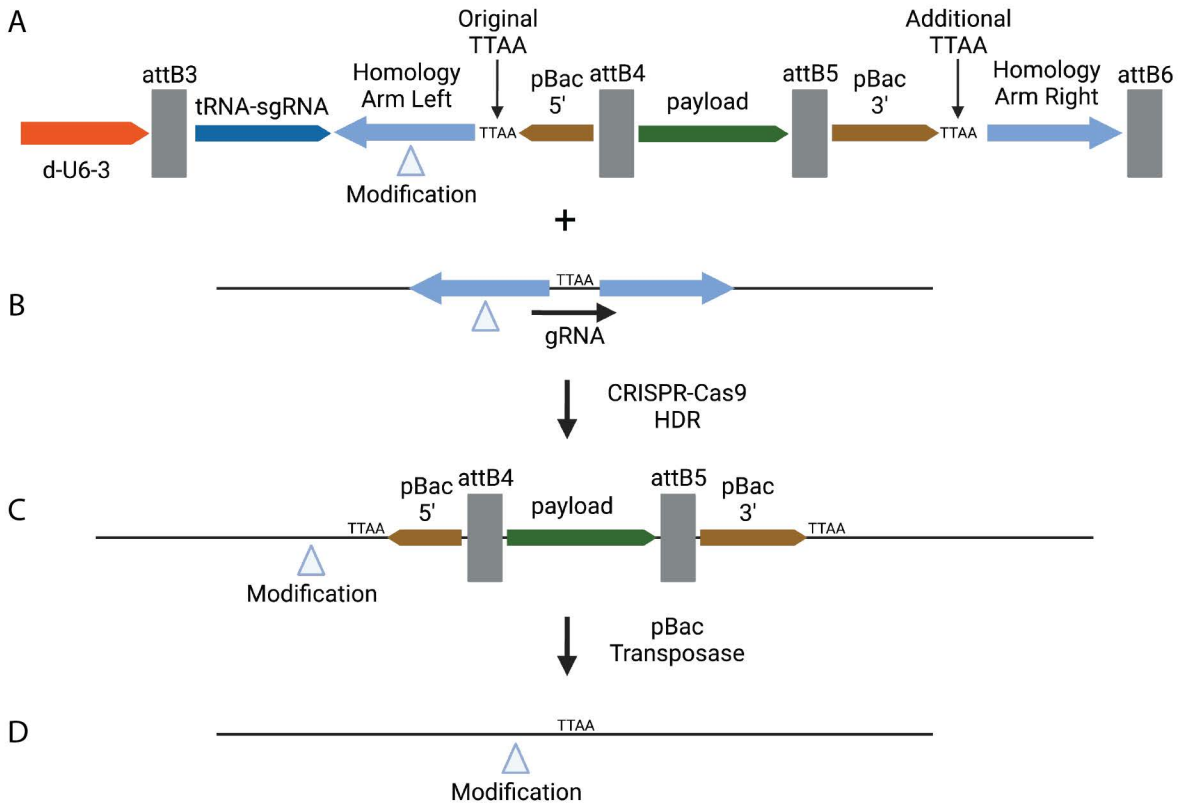
A
Original
TTAA
Additional
TTAA
attB3
tRNA-sgRNA
Homology
Arm Left
pBac
5'
attB4
payload
attB5
pBac
3'
Homology
Arm Right
attB6
d-U6-3
TTAA
TTAA
Modification
+
B
TTAA
gRNA
CRISPR-Cas9
HDR
C
pBac
5'
attB4
payload
attB5
pBac
3'
TTAA
TTAA
Modification
pBac
Transposase
D
TTAA
Modification

Figure 5

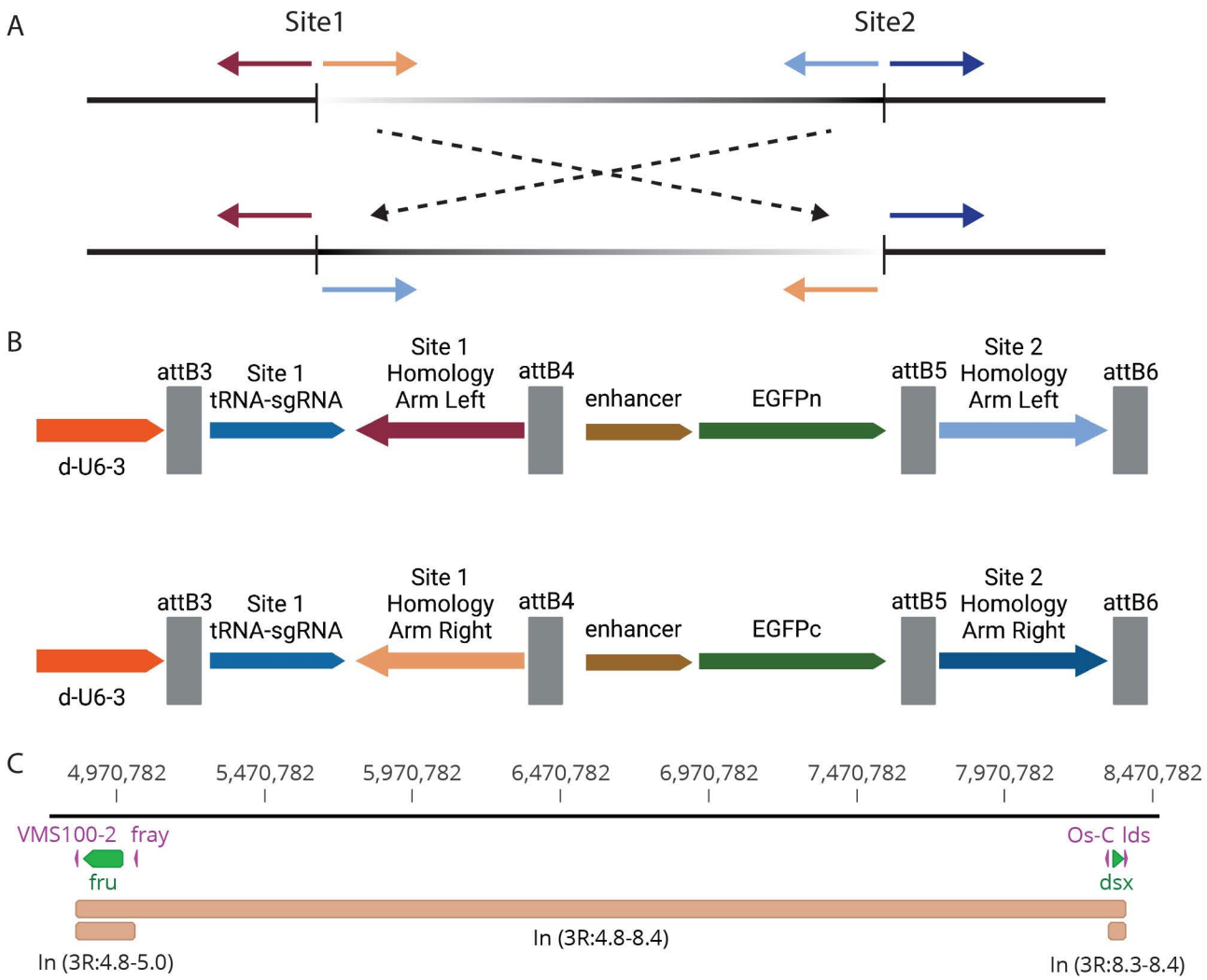
A
Site1
Site2
B
attB3
Site 1
tRNA-sgRNA
Site 1
Homology
Arm Left
attB4
enhancer
EGFPn
attB5
Site 2
Homology
Arm Left
attB6
d-U6-3
attB3
Site 1
tRNA-sgRNA
Site 1
Homology
Arm Right
attB4
enhancer
EGFPc
attB5
Site 2
Homology
Arm Right
attB6
d-U6-3
C
4,970,782
5,470,782
5,970,782
6,470,782
6,970,782
7,470,782
7,970,782
8,470,782
VMS100-2
fray
fru
Os-C
lds
dsx
In (3R:4.8-5.0)
In (3R:4.8-8.4)
In (3R:8.3-8.4)

Supplementary Figure 1

Supplementary Figure 2

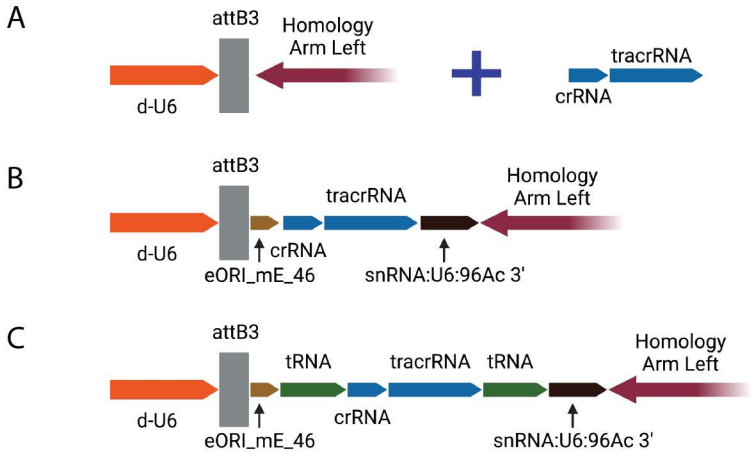

Construct form	Construct	Number injected	Number Fertile	Number Positive	Efficiency (%)
A	CG42402 + gRNA	250	17	3	18
B	gRNA-CG42402	285	17	3	18
C	tRNA-gRNA-tRNA-CG42402	283	25	12	46

Supplementary Figure 3

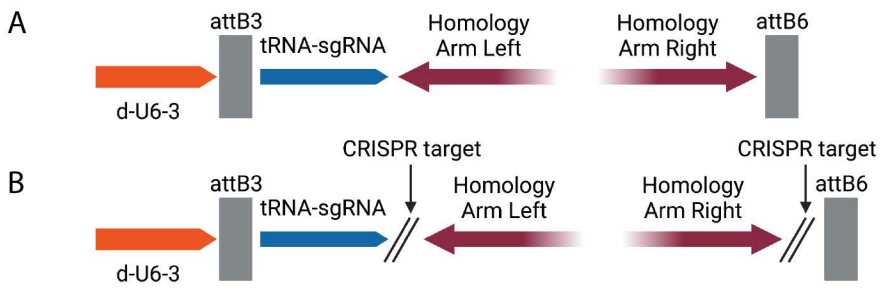

Construct Form	Construct	Left Homology Arm Length	Right Homology Arm Length	Number injected	Number Fertile	Number Positive	Efficiency (%)
A	l(2)gl	250	250	265	65	1	2
A	l(2)gl	1000	1000	265	45	0	0
B	CRISPR-l(2)gl-CRISPR	250	250	250	37	0	0
B	CRISPR-l(2)gl-CRISPR	1000	1000	280	61	0	0
A	Ir41a	250	250	260	64	25	39
A	Ir41a	600	600	260	46	12	26
B	CRISPR-Ir41a-CRISPR	250	250	255	53	10	19
B	CRISPR-Ir41a-CRISPR	250	600	280	47	4	9

Supplementary Figure 4

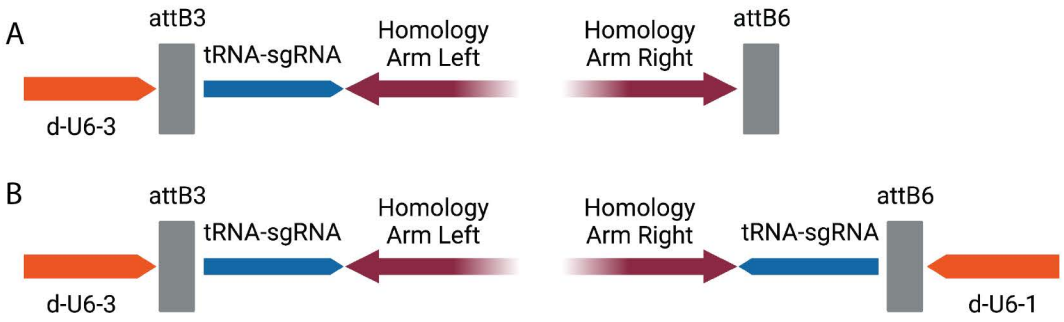

Construct form	Construct	Number injected	Number Fertile	Number Positive	Efficiency (%)
A	dU6-3-Tm1	240	27	13	48
B	dU6-3-Tm1-dU6-1	260	31	8	26
A	dU6-3-Osi2	250	49	26	53
A	dU6-3-Osi2	250	72	10	36
A	dU6-3-Osi2	275	82	10	14
B	dU6-3-Osi2-dU6-1	275	44	19	43

Supplementary Figure 5

A

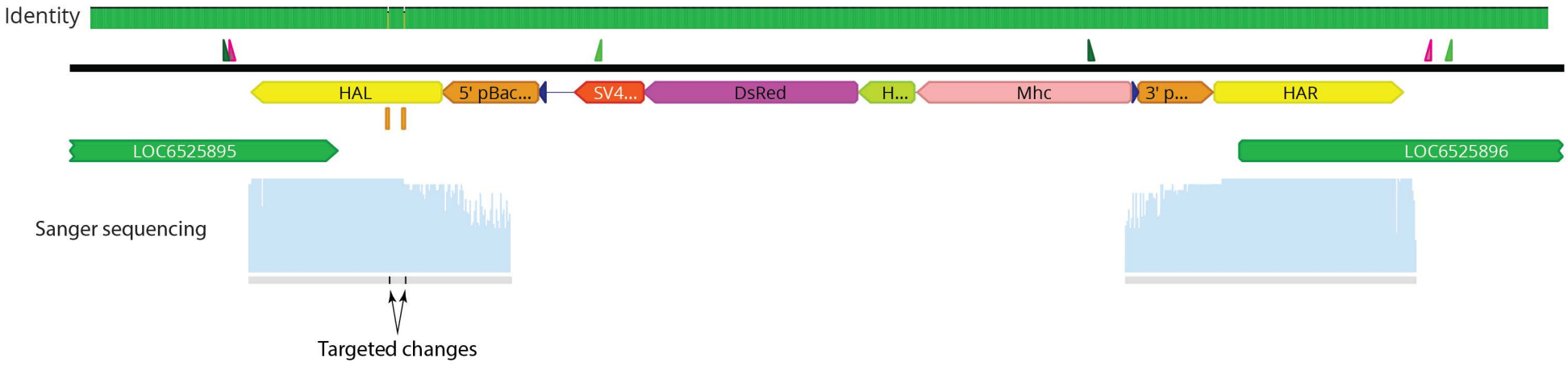

B

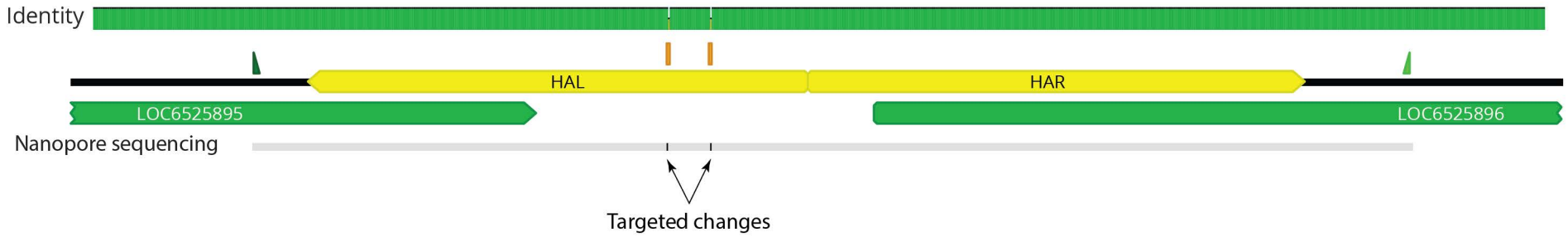

Supplementary Figure 6

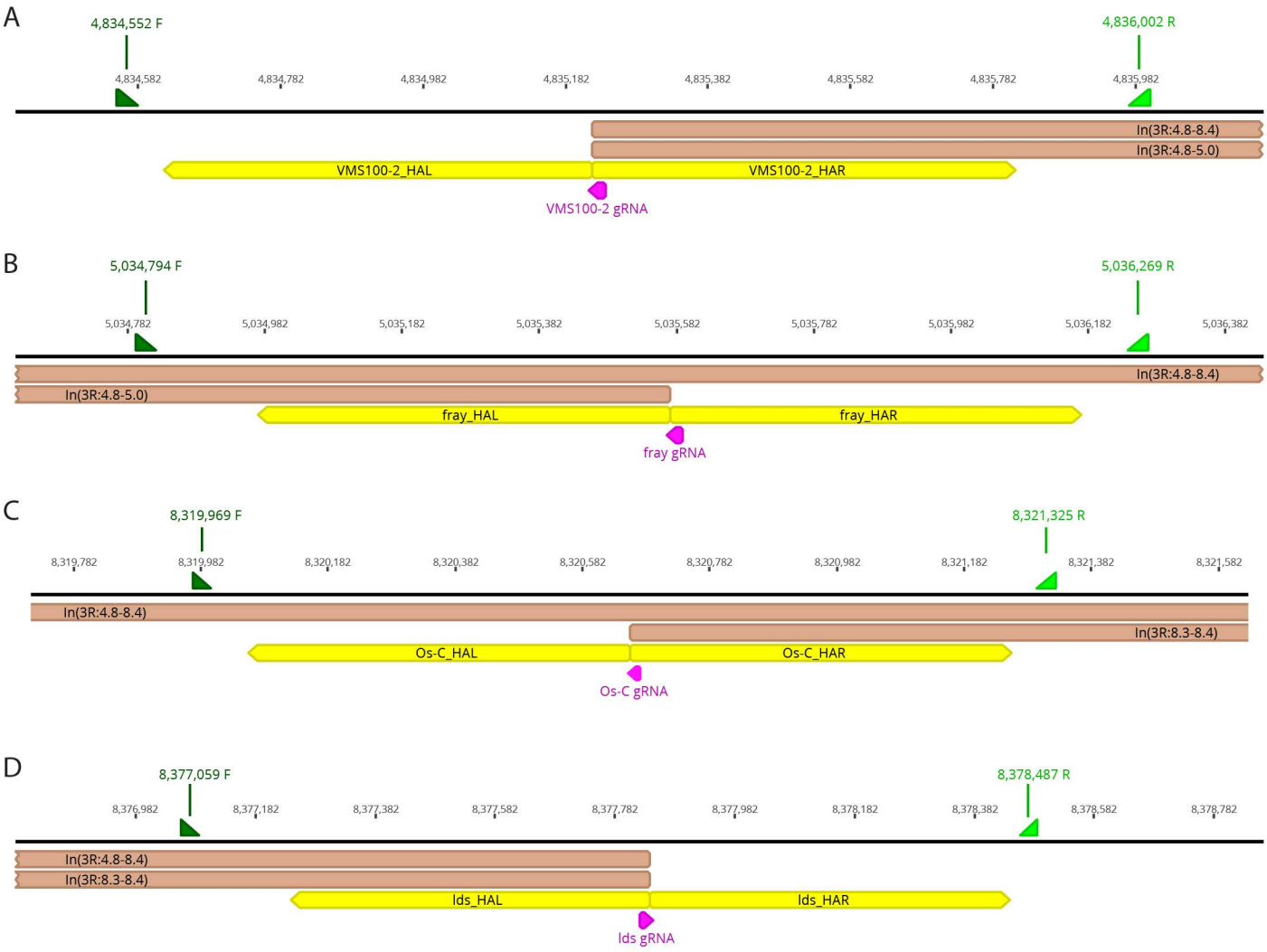
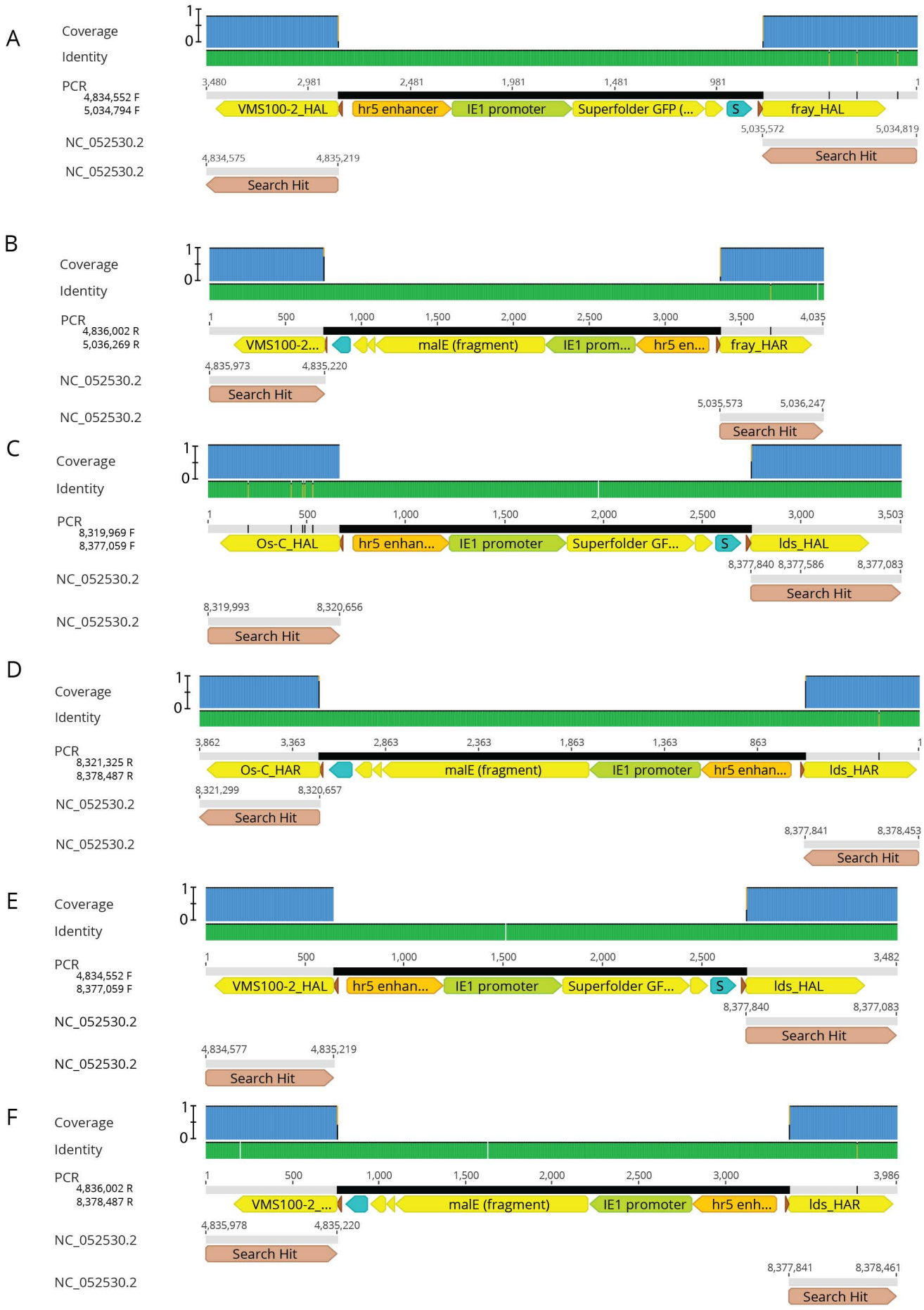
Supplementary Figure 7